

Proton channel models

Filling the gap between experimental data and the structural rationale

Amaury Pupo^{1,2}, David Baez-Nieto¹, Agustín Martínez¹, Ramón Latorre¹, and Carlos González¹

¹Centro Interdisciplinario de Neurociencia de Valparaíso; Facultad de Ciencias; Universidad de Valparaíso; Valparaíso, Chile; ²Doctorado en Ciencias mención Neurociencia; Universidad de Valparaíso; Chile

Keywords: proton channel, Hv1, homology model, molecular dynamics, function–structure relationship

Voltage-gated proton channels are integral membrane proteins with the capacity to permeate elementary particles in a voltage- and pH-dependent manner. These proteins have been found in several species and are involved in various physiological processes. Although their primary topology is known, lack of details regarding their structures in the open conformation has limited analyses toward a deeper understanding of the molecular determinants of their function and regulation. Consequently, the function–structure relationships have been inferred based on homology models. In the present work, we review the existing proton channel models, their assumptions, predictions, and the experimental facts that support them. Modeling proton channels is not a trivial task due to the lack of a close homolog template. Hence, there are important differences between published models. This work attempts to critically review existing proton channel models toward the aim of contributing to a better understanding of the structural features of these proteins.

Introduction

Although proton currents were identified in the 1980s in snail neurons and amphibian oocytes^{18–20} and later in mammalian,²¹ including human cells,^{22–24} the existence of voltage-gated proton channels was not unanimously accepted until the discovery of the genes encoding for human and murine Hv1 in 2006.^{25,26} Voltage-gated proton channels are expressed in many tissues,^{25–27} and they are involved in various physiological process. For example, they extrude protons from epithelial,²⁸ muscle, and neuron cells²⁹ and regulate airway surface liquid pH.²⁸ Additionally, they are required for histamine secretion by basophils,³⁰ reactive oxygen species production by the NADPH oxidase in phagocytes,^{29,31,32} sperm capacitation³³ and motility,³⁴ and B lymphocyte signaling.³⁵ Lastly, they are overexpressed in breast cancer metastasis³⁶ and have been observed to enhance ischemic brain damage.³⁷

Proton channels are made of a cytoplasmic N-terminus, a coiled-coil cytoplasmic C-terminal domain and four trans-membrane regions (TM 1–4), homologous to voltage-sensing domain (VSD) of other voltage-gated ion channels (Nav, Kv, and Cav channels) and the voltage-sensor-containing phosphatase (VSP).^{25,37} Hv1 channels lack the last two TM segments which constitute the pore forming domain of voltage-gated ion channels.^{25,26} Hv1 assembles as homodimers, which are stabilized by interactions of the C-terminal coiled-coil domains.^{38–40} Monomeric channels, obtained by deletion or disruption of C-terminal domains are functional, indicating that permeation occurs within an individual VSD.^{38,39} The Hv1 monomer has a dual function: it gates the proton current and also serves as the proton conduction pathway, not requiring accessory proteins.⁴¹ Hv1 has voltage and time dependent gating like other “classical” ion channels,⁴² is extremely selective ($P_{\text{H}}/P_{\text{Na}} > 10^6$),⁴³ voltage dependence is strictly coupled to the pH gradient across the membrane,⁴² and both gating and conductance show a strong temperature dependence.^{44,45}

Function–structure relationships of Hv1 channels were first inferred based on the conserved features of VSD domains. Voltage sensitivity in the VSD is conferred by a series of highly conserved positions for charged residues. Particularly, S4 contains several repetitions of a basic amino acid (mainly R) followed by two hydrophobic residues.^{46–48} Hv1 channels have three of those triplets repeats^{25,26} and motion of S4 during activation has been reported^{49,50} similarly as previously observed in other voltage-activated channels.^{2,51–53} These three arginines contribute to most, if not all, of the gating charges in Hv1 channels.^{50,54} In other VSD, as S4 moves, its arginines participate in salt bridges with intracellular and extracellular charge clusters, which are separated by the constriction at the charge transfer center.^{55–59} Something equivalent is expected to occur in Hv1 channels, but while the structure of the open state of the channels remains unknown, the detailed atomic interactions that define their function can only be inferred by molecular models.

There are seven curated Hv1 proteins in Uniprot⁶⁰: the Hv1 from *Ciona intestinalis*, *Xenopus laevis*, *Xenopus tropicalis*, *Danio rerio*, *Gallus gallus* (chicken), *Mus musculus* (mouse), and *Homo sapiens*. Aligned sequences are shown in **Figure 1**. Although N-terminal domain is highly variable between Hv1 molecules, the membrane domain (particularly the four trans-membrane

*Correspondence to: Carlos González; Email: carlos.gonzalezl@uv.cl
Submitted: 02/24/2014; Revised: 03/24/2014; Accepted:
03/25/2014; Published Online: 04/22/2014
<http://dx.doi.org/10.4161/chan.28665>

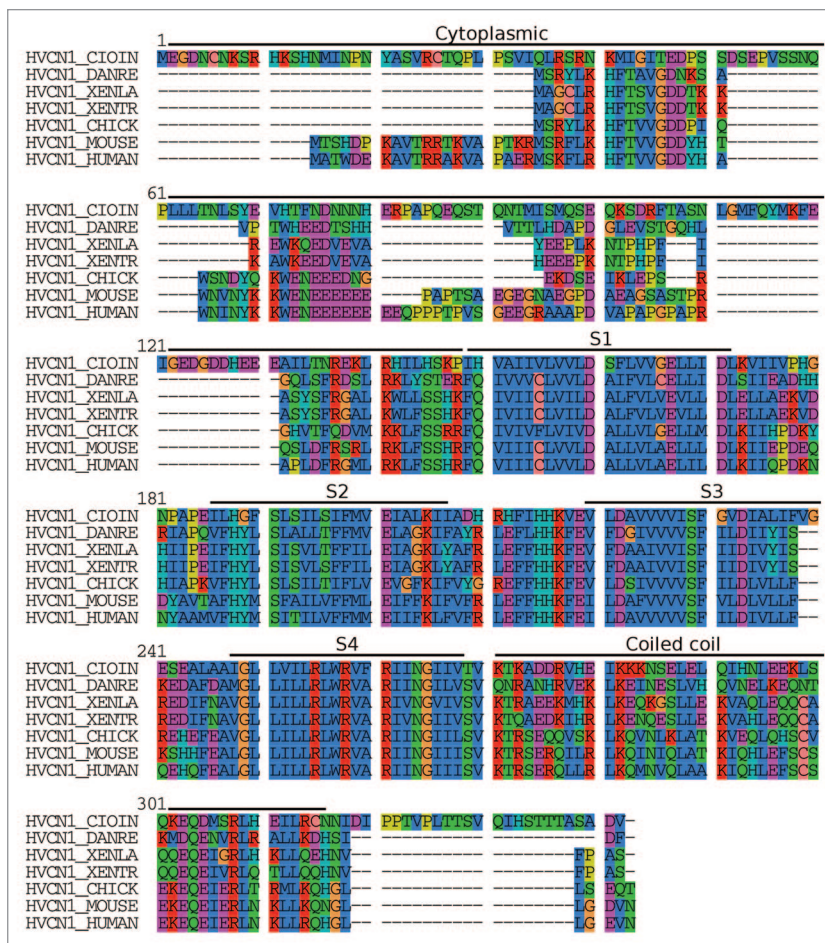


Figure 1. Alignment of Hv1 sequences from *Ciona intestinalis* (HVCN1_CIOIN), *Danio rerio* (HVCN1_DANRE), *Xenopus laevis* (HVCN1_XENLA), *Xenopus tropicalis* (HVCN1_XENTR), *Danio rerio* (HVCN1_DANRE), *Gallus gallus* (HVCN1_CHICK), *Mus musculus* (HVCN1_MOUSE), and *Homo sapiens* (HVCN1_HUMAN). Uniprot names are used. The cytoplasmic N-terminal domain, the four trans-membrane segments, and the coiled-coil region are labeled. Residues are colored by type following clustalx conventions.

α -helices) and the coiled-coil region of the C-terminal domain are well conserved.

In the present work we review the different structural models of voltage-gated proton channel proposed to date, how they were obtained, their assumptions and predictions, with emphasis in the experimental data which support them. We compare all their atomic coordinates and highlight the most significant structural differences.

We start by devoting the whole next section to a common and difficult problem in the modeling of membrane proteins structures: finding good templates.

Modeling Proton Channel by Homology, in Search of a Good Template

Until very recently, only the structure of the C-terminal domain of Hv1 was known. Li et al.⁶¹ obtained the crystallographic structure at 2.0 Å of resolution. They found that

the two monomers form a dimer via a parallel α -helical coiled-coil. The secondary structure of C-terminal increase with a pH decrease and remains α -helical and dimeric irrespective of pH.⁶¹ This C-terminal domain is important for the selective localization of Hv1 in the intracellular compartment membranes rather than the plasma membrane of HeLa cells.

Takeshita et al.⁶² just published the structure of a chimeric version of murine Hv1 channel in the closed conformation. This is a breakthrough in the field, which will help to understand some of the properties of Hv1 channel. Unfortunately, as there is not yet a structure of the open conformation of the channel, then function–structure relationship studies of processes such as permeation will still be based on molecular models. Homology modeling is the most accurate computational method for protein structure prediction,^{63,64} provided that good homolog templates are available. The finding of such templates, plus the subsequent sequence alignment, is the most important step in homology modeling.^{65–68} Up until February 2014 the structures of membrane proteins represent less than 3% of all structures in the PDB, the finding of a good template for any membrane protein, including proton channels, can be a daunting task. Due to the dynamic nature of the structure of voltage-dependent ion channels it is frequent that just one of the two, or multiple, functional relevant conformations of a given channel has an experimentally resolved structure. This results in the singular situation when a potential template with 100% of identity (indeed the same protein, but in other conformation) is not useful to model all the target structure. In the case of the open conformation of Hv1 channel potential templates in an activated, up, or open conformation must be found.

The most common way to search for templates is to perform a BLAST⁶⁹ with the target sequence against the PDB database. By doing a more sensitive DELTA-BLAST⁷⁰ homolog search against PDB, using the membrane domain of each of the 7 manually annotated Hv1 sequences in Swissprot (see Fig. 1), 15 potential templates appeared (Table 1). The structure of Na_vCt voltage-gated sodium channel (4BGN) can be rapidly discarded due to its poor resolution (9 Å). All 5 Ca_vAb voltage-gated calcium channel structures¹¹ in Table 1 (4MS2, 4MVQ, 4MVU, 4MVZ, and 4MW3) were obtained by point mutations in the selectivity filter of Na_vAb, sharing exactly the same VSD domain between them and with Na_vAb. There are four structures of Na_vAb acting as possible templates, two structures of the wild type (4EKW and 4MW8), the mutant M221C (3RW0), and the mutant I217C (3RVY). Those four structures have the same VSD domain, being 3RVY the one with the best resolution and with a R free factor as good as 3RW0 (Table 1). The two structures of the Kv1.2-Kv2.1 paddle chimera channel,

Table 1. Potential templates for homology models of proton channels

Possible templates	PDB code	Resolution (Å)	R free	Channel conformation	Reference
NavCt voltage-gated sodium channel	4BGN	9.00	0.473	Relatively open and closed	16
NavRh voltage-gated sodium channel	4DXW	3.05	0.268	Closed, but depolarized VSD	17
CavAb voltage-gated calcium channel ^a	4MS2	2.75	0.255	Open	11
CavAb voltage-gated calcium channel ^a	4MVQ	3.40	0.313	Open	11
CavAb voltage-gated calcium channel ^a	4MW3	3.30	0.267	Open	11
CavAb voltage-gated calcium channel ^a	4MVZ	3.30	0.280	Open	11
CavAb voltage-gated calcium channel ^a	4MVU	3.20	0.263	Open	11
NavAb voltage gated sodium channel	4MW8	3.26	0.314	Open	11
Shaker Kv1.2 potassium channel ^b	2A79	2.90	0.252	Open	3
Shaker Kv1.2 potassium channel	3LUT ^c	2.90	0.221	Open	7
NavAb voltage-gated sodium channel (I217C)	3RVY	2.70	0.273	Closed pore conformation with activated VSD	8
Kv1.2-Kv2.1 paddle chimera channel	2R9R	2.40	0.244	Open	14
NavAb voltage-gated sodium channel (M221C)	3RW0	2.95	0.272	Closed pore conformation with activated VSD	8
NavAb voltage-gated sodium channel (WT)	4EKW ^d	3.21	0.322	Inactivated channel, activated VSD	15
F233W mutant of the Kv1.2-Kv2.1 paddle chimera channel	3LNM	2.90	0.247	Open	9
KvAP potassium channel ^e	1ORS	1.90	0.251	Open	10

^aObtained by point mutations in the selectivity filter of NavAb channel. The VSD domains are the same of NavAb. ^bA significant portion of the VSD domain is not well resolved. ^cThis structure was obtained from the original diffraction data from which 2A79 was obtained, but applying a novel normal-mode-based X-ray crystallographic refinement method. So 3LUT is an improved version of 2A79. ^dSame VSD of 2R9R and 3RW0. ^e1ORS does not appear as a potential template in the delta blast search against PDB using the membrane domains of Hv1 as query sequences.

namely the wild type (2R9R) and the F233W mutant (3LNM), from which 2R9R with 2.4 Å is a clear template choice. There are also two structures of Shaker Kv1.2 potassium channel as potential templates, 2A79 and 3LUT (Table 1). Both structures were obtained from the same diffraction data, but Chen et al.⁷ applied a normal-mode-based X-ray crystallographic refinement method to improve the 3LUT model. Although at a lower resolution (3.05), the structure of NavRh voltage-gated sodium channel (4DXW) can be also considered among the suitable templates. Curiously, the structure of the KvAP potassium channel (1ORS) does not appear as a probable template in our DELTA BLAST analysis, but it was included in Table 1 because it had been used to model the Hv1 channel by different groups (Table 4). Thus, from the preliminary analysis of structures in Table 1, 5 potential templates for membrane domain models of Hv1 emerged: 1ORS, 2R9R, 3LUT, 3RVY and 4DXW (in alphabetical order). None of the VSD domains from these proteins are more than 30% identical to proton channel membrane domains (Table 1). The VSD domain from NavRh voltage-gated sodium channel (4DXW) has the highest identity

values, ranging from 26% to 29%, and the Kv1.2-Kv2.1 paddle chimera (2R9R) has the lowest, from 11% to 14%. This was found to be a common situation in the modeling of membrane proteins, then similarity, which seems to be a more relaxed criterion, has been taken in account in order to find a suitable template.⁶³ VSDs of NavAb (3RVY) and NavRh (4DXW) have more than 50% of similarity with membrane domains of proton channels (Table 2), KvAP (1ORS) has more than 40% and both Kv1.2-Kv2.1 paddle chimera (2R9R) and the Shaker Kv1.2 (3LUT) have as similarity values close to 30%. Based on sequence similarity the strongest candidates as templates are NavRh (4DXW) and NavAb (3RVY), but it should be recalled that 4DXW is the only one out of the 5 structures with more than 3 Å of resolution.

It is a fact that homology models against low sequence identity templates (less than 30%, which include all potential templates above) tends to be inaccurate.^{71,72} Another source of uncertainty in modeling proton channels is the large structural divergence between potential templates (Table 3). Selecting one template over another, together with variations in the nontrivial sequence

Table 2. Percentage of similarity between membrane domains of Hv1 sequences and VSD domains of potential templates

Hv1 sequences*	Identity ^a					Similarity ^b				
	1ORS_C	2R9R_B	3LUT_B	3RVY_A	4DXW_A	1ORS_C	2R9R_B	3LUT_B	3RVY_A	4DXW_A
HVCN1_CIOIN	17	11	16	22	26	43	30	32	51	53
HVCN1_XENLA	14	14	19	24	28	45	34	34	54	56
HVCN1_XENTR	15	14	19	22	29	45	34	34	54	56
HVCN1_DANRE	19	14	21	19	27	45	32	33	53	55
HVCN1_CHICK	17	14	20	19	26	46	32	32	53	55
HVCN1_MOUSE	15	13	18	23	28	44	32	32	53	56
HVCN1_HUMAN	14	13	19	21	29	44	36	34	52	55

Templates VSD domains are referred as PDB code and the chain name. *Uniprot names are used. ^a%Identity = 100. *(Identical residues / Length of the shortest sequence). ^b%Similarity = 100. *(Similar residues / Length of the shortest sequence). Six similarity groups are considered, following the classification proposed by Livingstone et al.⁷⁹: Aromatic (F, Y, W), Aliphatic (V, I, L), Charged positive (R, K, H), Charged negative (D, E), Polar (N, Q), and Small (A, T, S).

Table 3. Structural comparison of VSD domains from potential templates

Structures	1ORS_C	2R9R_B	3LUT_B	3RVY_A	4DXW_A
1ORS_C	–	–	–	–	–
2R9R_B	5.4	–	–	–	–
3LUT_B	6.6	9.7	–	–	–
3RVY_A	8.4	7.2	8.1	–	–
4DXW_A	9.9	7.4	8.9	4.9	–

RMSD values (Angstroms) between Ca atoms of aligned residues in the paired VSD structures are shown. Each structure is identified by its PDB code plus the chain name from which the VSD domain is extracted. There is a significant structural diversity between the VSD domains being the couples 3RVY plus 4DXW and 1ORS plus 2R9R the most similar pairs, but still far from structural equivalence.

alignments between proteins with these low identities, leads to very different models, which then need strong experimental validation.

Current Homology Models for Voltage-Gated Proton Channel (Hv1)

There are 8 published models of the membrane domain of proton channel, 7 in the open^{5,6,12,13} and one in the closed conformation⁵ (Table 4). Unsurprisingly, most of the models are for the human Hv1.^{6,12,13} From the potential templates previously analyzed, the following 3 have been used: KvAP, Na_vAb, and the Kv1.2-Kv2.1 paddle chimera, which is the most popular being used in 6 of the 7 open models.

Musset et al.⁷³ published the first homology model of the proton channel, using both KvAP (1ORS) and the paddle chimera (2R9R) as templates. This models allow them to hypothesize that high-affinity Zn²⁺ binding occurs at the dimer interface between

pairs of His residues from Hv1 monomers, because H140 and H193 are too far in a monomer (–14 Å). This model was discarded and replaced later by R2D and R3D models¹³ (see Table 4) by the same authors, which explains why it is not included in a more detailed analysis in the current review. Recently, Takeshita et al.⁶² found the Zn²⁺ binding site to be located in each single monomer, constituted by residues equivalents to human Hv1 H140, H193, E119, and D123.

Hv1A and Hv1B Models

Ramsey et al.⁶ also used KvAP and the paddle chimera as templates, but in this case Hv1A was modeled vs KvAP and Hv1B vs the paddle chimera (Table 4). A structural-profile sequence-profile alignment is done in order to obtain the best correspondence. The resulting alignments are shown in Figure 2A. In these alignments, R3 is equivalent to R4 residues of KvAP and Kv1.2–2.1. The structural models were equilibrated in a hydrated POPC bilayer by 320 ns of coarse-grained molecular dynamics, followed by 1 ns of all atom equilibration with restrained heavy atoms, and finally by 20 ns of restrain-free all atom molecular dynamics. Resulting models are shown in Figure 3A and B. The VSD domain of NaChBac channel was modeled with a similar procedure to be used as a reference for the molecular dynamics analysis.

In order to address the involvement of tritable residues in proton permeation through the channel Ramsey et al.⁶ identify candidates residues, based on their conservation in the sequences of human, mouse and Ciona Hv1, and neutralized them. Five mutants of human Hv1 were obtained, namely D174A, E153A, K157A, D185A, and D112A. Whole cell voltage clamp

Figure 2 (opposite page). Reconstruction of the alignments used to build the published homology models. All the alignments are putted together to form a bigger one. In some cases just the alignment of the four trans-membrane segments are reported, then the loops are missing. (A) Alignments of the membrane domain of human Hv1 vs 1ORS (for model Hv1A) and vs chain B of 2R9R (for Hv1B).⁶ (B) Two different alignment of human Hv1 vs 2R9R_B. The alignments are equivalents, except in the S4, where a gap is inserted to make R1 of Hv1 equivalent to R2 of the chimera.¹² (C) The alignment of membrane domain of human Hv1 against 1ORS, 2R9R_B and 3RVY_A simultaneously. Alignments for R2D and R3D are equivalents, except in the S4 region: R1 from R3D is aligned with R1 of 1ORS and 3RVY and with R2 of 2R9R, while in R2D S4 is moved 3 residues to the right, so the third ARG of Hv1's S4 is equivalent to R4 in 1ORS and 3RVY and to K5 in 2R9R.¹³ (D) Alignments for *Ci-Hv1 open* vs 2R9R and *Ci-Hv1 closed* vs the homology model of Kv1.2 in the closed state from Pathak et al.²

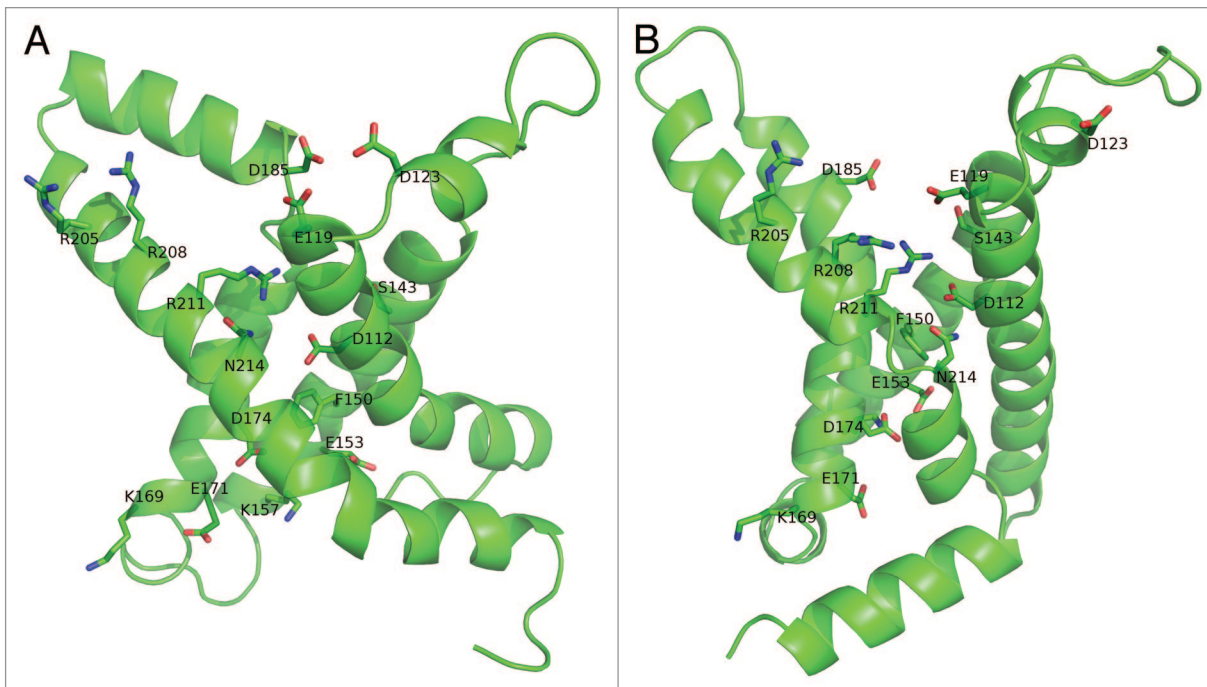


Figure 3. Hv1A and Hv1B models. Structures are represented in cartoon and side chains of highly conserved residues are shown in sticks and labeled. (A) Hv1A. (B) Hv1B.

experiments were performed in HEK 293, HM1, or 293T cells expressing the wild-type protein or mutants. All the single and double and several of the triple mutants tested present robust currents, together with the result that His neutralization (H140A/H193A and H167A/H168A double mutants) does not prevent conduction, leads them to conclude that no titratable residue was directly involved in permeation. Subsequently they proposed the existence of a water wire, by which protons are transferred through a Grothuss type mechanism. The existence of a stable molecular wire in the molecular dynamics simulation of at least the Hv1A model and Hv1A mutants D112N and E153N reaffirms this assumption. This water wire does not appear in the VSD domain of NaChBac models, or in previous simulations of Kv 1.2–2.1 paddle chimera, KvAP, and Mlotik. None of the neutralizing mutations affects voltage dependence or $V_{\text{threshold}}-\Delta\text{pH}$ slope. E153A and D174A have been observed to significantly shift voltage activation potential toward negative potentials, while D185A and D112A shift it toward positive potentials. This is in correspondence with the localization of E153 and D174 in the internal (cytoplasmic) negative cluster (see Fig. 3A and B), which should stabilize the closed conformation by means of electrostatic interactions with the voltage sensor and with the localization of D112 and D185 in the external negative cluster (Fig. 3A and B), which should participate in the stabilization of the open conformation. In Hv1A such stabilization can be explained by interactions of R211 mainly with D112. R205 and R208 both point toward the extracellular compartment (Fig. 3A), interacting with lipid head groups and solvent. In addition to R211 interaction with D112 and S143, R208 can interact with E119 in Hv1B

and R211 is close enough to D185 to establish an electrostatic interaction (Fig. 3B).

R1-Hv1 and R2-Hv1 Models

R1-Hv1 and R2-Hv1 (Fig. 4A and B) human proton channel models were proposed by Wood et al.¹² (Table 4). As shown in Figure 2B, R1 aligns to position R1 of the paddle chimera (actually a GLN) in R1-Hv1, while this residue is aligned to position R2 in R2-Hv1. This is essentially a theoretical work, where a stable water wire formation can be seen in R1-Hv1 and to a lesser degree in R2-Hv1 through molecular dynamics simulations.

The initial models were created from the alignments shown in Figure 2B¹² using Modeller (Fig. 4A and B). Then, an all atom molecular dynamics of 200 ns for R1-Hv1 and R2-Hv1 and 135 ns for the mutant N214R R1-Hv1 was performed in a hydrated POPC bilayer. R1-Hv1 has a constriction region formed by hydrophobic residues V116, I146, and L147, roughly starting at the protein center and extending for about 5 Å toward the extracellular side. F150 is the intracellular facing residue closest to this hydrophobic cluster. N214 is positioned at almost the same level (Fig. 4A). Residues R208 and R211 have been observed to form salt-bridges with D123 and E119. D112 is in the intracellular compartment interacting mainly with water molecules and at approximately the same level as N214 and F150 (Fig. 4A).

During the molecular dynamics simulation, R211 goes from an initial extracellular compartment location (as can be seen in Fig. 4A) to the intracellular compartment (as reported in ref. 12). The initial position of R211 is expected from the

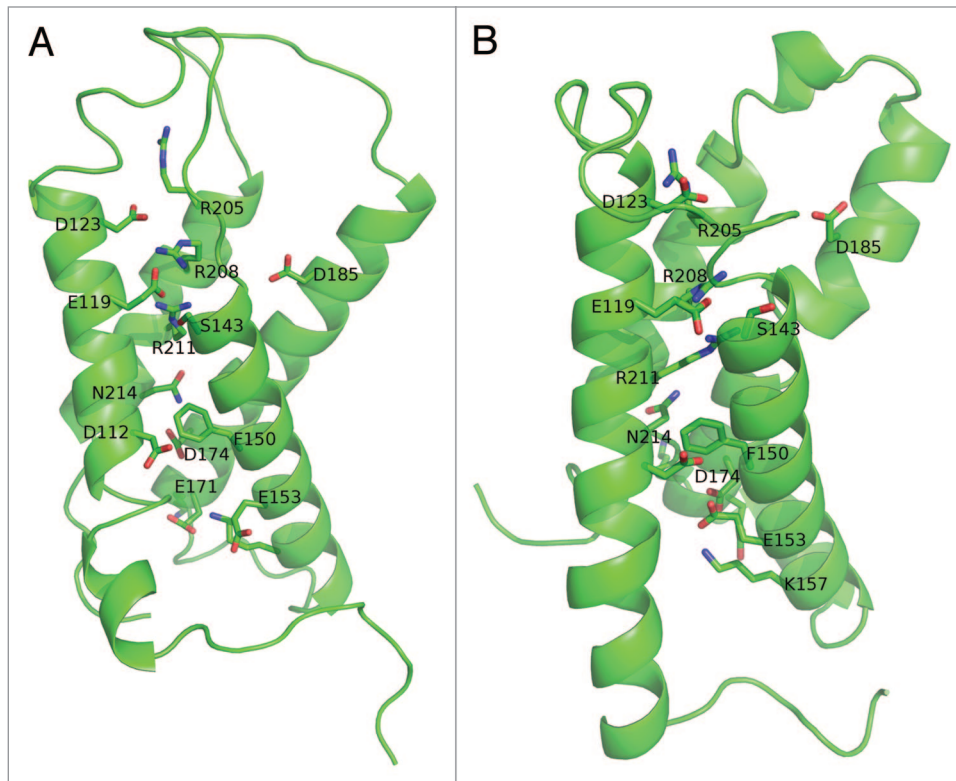


Figure 4. R1-Hv1 and R2-Hv1 models. Structures are represented in cartoon and side chains of highly conserved residues are shown in sticks and labeled. (A) R1-Hv1 structure used to initiate the MD simulations. (B) R2-Hv1 structure used to initiate MD simulations.

alignment (Fig. 2B) with the R4 position of the paddle chimera. This arginine interacts with the external negative cluster in 2R9R,¹⁴ over the hydrophobic core. It is important to point out that such a drastic change in functional residue localization is not common during homology model refinement through molecular dynamics. During the simulation R211 forms a salt bridge with D122 and R208 forms a persistent salt-bridge with E119.

R2D and R3D Models

Musset et al.⁷⁴ mutated 5 residues perfectly conserved in 21 Hv1 family members by their equivalents in the uncharacterized C15orf27 protein. Four mutants, namely, G215A, D185M, N214D, and S219P, showed large proton currents in whole cell voltage clamp. D112V was localized in the plasma membrane but conductance was not observed. This led to further mutations of D122 with unexpected result that 6 out of 7 tested mutations (D112 for H, K, N, S, A, and F) were selective for anions, as tested by the positive shift of V_{rev} in experiments where 90% of the bath solution was replaced by isotonic sucrose. Only the mutant D122E remained selective to protons. This suggests that the D112A mutant currents observed by Ramsey et al.⁶ were anionic currents. Musset et al.⁷⁴ proposed D112 to be the proton channel selectivity filter.

In order to explain newer experimental data, particularly the role of D112 as the proposed selectivity filter, Kulleperuma et al.¹³ dismissed the model previously reported by Musset et al.⁷³ and created two new models of the human Hv1, again using multiple templates (Table 4). Modeling based on multiple templates is often advantageous, but it is not easy to benefit from enlarging the number of templates when their local structures differ significantly⁷⁵ (Table 3). The result of a very careful and robust alignment procedure is shown in Figure 2C. As with R1-Hv1 and R2-Hv1 models, R2D and R3D alignments differ in the register of arginines in S4. R3D has its S4 aligned with 2R9R similar to Hv1B (Fig. 2A) and R2-Hv1 (Fig. 2B). S4 from R2D has a different alignment, with R3 aligned to K5 position of the paddle chimera. Because K5 and R6 form ionized hydrogen bonds with the internal negative cluster in 2R9R,¹⁴ under the hydrophobic core, R211 is expected to be intracellular-accessible in the R2D model. This is in correspondence with the alignment of R211 with positions R4 of K_vAP^{10} and R4 of $Na_vAb.^8$

The 5 best models obtained with Modeller per alignment were subjected to 25 all atom molecular dynamic simulations in hydrated octane, at 300K for 100 ns, without any structural restraint. Since model variation within R2D and R3D simulations was found to be trivial, the structures from the top five models were combined for each R2D and R3D. In R2D model D122 is facing R208 (Fig. 5A), while in R3D is facing R211 (Fig. 5B). Both models were submitted to an analysis of

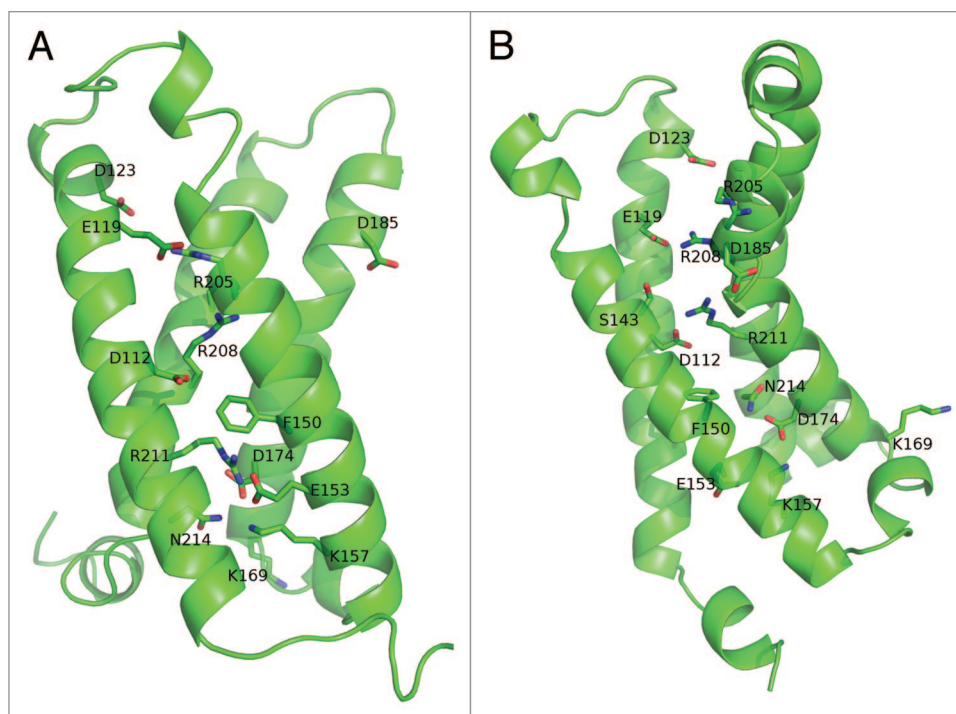


Figure 5. R2D and R3D models. Structures are represented in cartoon and side chains of highly conserved residues are shown in sticks and labeled. (A) R2D. (B) R3D.

structural divergence during the MD simulations, with emphasis in monitoring the size of the most populated structural cluster and the change in the number of α -helical residues. Both models had a larger structural divergence than that of the templates, but R3D had a significantly larger divergence than R2D. Both models have two networks of salt-bridges, one internal and the other external. The external network of R2D is formed by R205 and R208 in S4, E119 and D112 in S1, and D185 in S3 while its internal network by R211 in S4, K157 and E153 in S2, and D174 and E171 in S3. The external salt-bridge network is formed in R3D by residues D112, R211, E119, and R208, but its internal network is missing. These results suggest that R2D is a better model, then its MD simulations were extended up to 200 ns for each of the 125 replicas.

A stable water wire can be formed in the molecular dynamics of the R2D model, whether in hydrated octane or in a hydrated lipid bilayer (four 100 ns all atom MD starting from different conformations of R2D). Pore hydration is modulated by two constriction sites formed by the interacting pairs D112–R208 and R211–F150. While the pair R211–F150 is disrupted 87% of the simulation time, the D112–R208 interaction is broken just 10% of the time. Water wire can only be formed when the previous pairs are not interacting. Events of disruption of D112–R208 pair and subsequent water wire formation can last longer than 1 ns.

In order to estimate the energetics of ion permeation in the proton channel, Kulleperuma et al.¹³ used continuum electrostatic calculations to compute the static field for the transfer of a positive point charge through the water filled state of the pore. In R2D, the static field cancels out throughout the narrowest region

of the pore which contains D112 and R208. Upon neutralization of residue D112, the static field increases by ~ 10 kcal/mol in the narrow region of the pore, due to the unpaired positive charge in R208. The behavior of D112 during molecular dynamics simulations are in correspondence with its proposed role as the Hv1 selectivity filter.^{74,76}

R2D model was used by Morgan et al.,⁷⁶ who performed a “selectivity filter scanning” introducing Asp residues at each position along S1 from 108 to 118 in a D112A background. Proton conduction was only restored with Asp or Glu at position 116. The D112V/V116D resembled WT in selectivity, kinetics, and Δ pH-dependent gating. A model of the D112V/V116D mutant was built over the R2D model. Molecular dynamic simulations indicate that D116 form a salt bridge with R205 and/or R206. In contrast to WT simulations water pathways was observed in all configurations of D112V/V116D mutant, which is consequence of a greater pore width. Interestingly average pore hydration in molecular dynamics was very similar for proton selective (WT and D112V/V116D), anion permeable (D112V/V116S and D112S) and no conducting mutant (D112V),⁷⁶ indicating that the average hydration profile is not a good predictor of selectivity or permeation. On the other hand, static field analysis due to the transfer of a positive charge throughout the channel agrees with the experimental results, as non-conducting and anion permeable mutants have a higher energetic barrier than WT and D112V/V116D.

Arguably, R2D is the best computational validated model so far. The ability of R2D model to explain the role of D112, as the proposed selectivity filter increases its value as a probable and useful model. In R2D model, R211 is in the intracellular compartment, which makes it accessible from the cytoplasmic

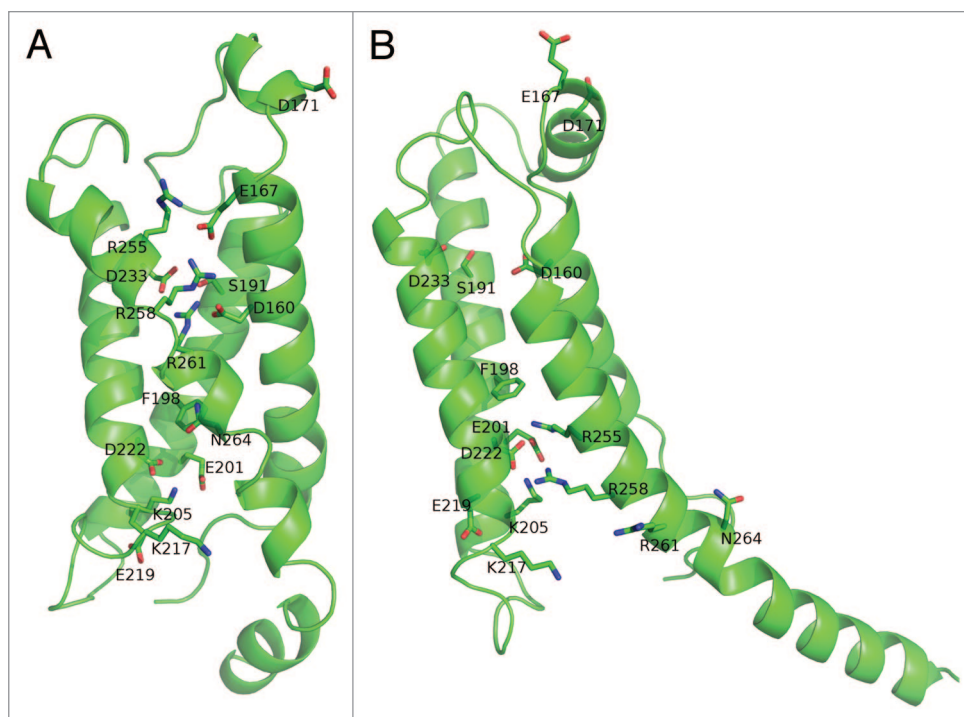


Figure 6. Ci-Hv1 models. Structures are represented in cartoon and side chains of highly conserved residues are shown in sticks and labeled. **(A)** *Ci-Hv1 open*. **(B)** *Ci-Hv1 closed*.

side, as well as R205 and R208 should be extracellularly accessible in the open channel conformation. It is clear that in the R205H, R208H and R211H mutants (done in an Zn^{2+} insensitive background: H140A/H193A/K221stop) positions 205 and 208, but not 211 are externally accessible to Zn^{2+} ions in the open conformation, while only H211, (but neither H205 or H208) is internally accessible. A similar result is observed in the D112V/V116D/R211H mutant.⁷⁶

The problem with the previous accessibility experiments is illustrated in reports such as Gonzalez et al.,⁵⁴ clearly showing that mutations of Arg residues in S4 alter the extent of S4 movement due to the need to readjust the network of electrostatic interactions, which stabilize the open and/or the closed conformations. Therefore, it is always advisable to mutate a nearby residue, but not the arginines in the voltage sensor.

Ci-Hv1 Models

Chamberlin et al.⁵ differs from the previous reports of proton channel models in more than one way. First, they modeled the *Ciona intestinalis* and not the human protein. Since the *Ciona intestinalis* membrane domain and that of the human share a 52.1% of identity and a 66.9% of homology, the structure-function relationships in proton channel are expected to be equivalent between both species. Second, apart from modeling the open conformation (see Table 4; Fig. 6A) they provided the first model of the closed conformation of a proton channel (*Ci-Hv1 closed*, represented in Fig. 6B). Until the recent resolution

of the structure of mHv1cc,⁶² this model was the only proposal about the structure of the closed conformation of Hv1. For the open conformation (model *Ci-Hv1 open*) the 2R9R coordinates of the paddle chimera was used as template, while in a bold move they use several models of the VSD of Kv1.2 in the closed state as templates (see Table 4). This template shares approximately a 17% of identity with Ci-Hv1.

The S4 alignment of *Ci-Hv1 open* and 2R9R (Fig. 2D) is similar to the ones in Hv1B (Fig. 2A), R2-Hv1 (Fig. 2B) and R3D (Fig. 2C). This model was built with ROSETTA-Membrane/Homology tools and then equilibrated in a hydrated DMPC lipid bilayer. All atom molecular dynamics runs of 100 ns were performed.

Through a thermodynamic mutant cycle analysis Chamberlin et al.,⁵ found that the interactions E201-R255, E201-R258, D222-R255, and D222-R258 stabilize the closed conformation, while interactions E167-R255, E167-R258, and D233-R258 stabilize the open conformation. It is interesting to note that although D160 is interacting with both R258 and R261 in *Ci-Hv1 open*, D160 does not show significant $\Delta G_{\text{coupling}}^0$ in any of the double mutants. As pointed out by the authors, thermodynamic mutant cycle analysis tends to yield more accurate results with Q(V) curves than with G(V).⁷⁷ It would be interesting try to reproduce these results with gating charge vs. voltage curves in proton channel, as observed by the research group led by Carlos Gonzalez (unpublished results).

Both the open and closed models are consistent with the interaction pairs identified, indicating that there is a strong correspondence between experimental and calculated $\Delta\Delta G_{\text{coupling}}^0$,

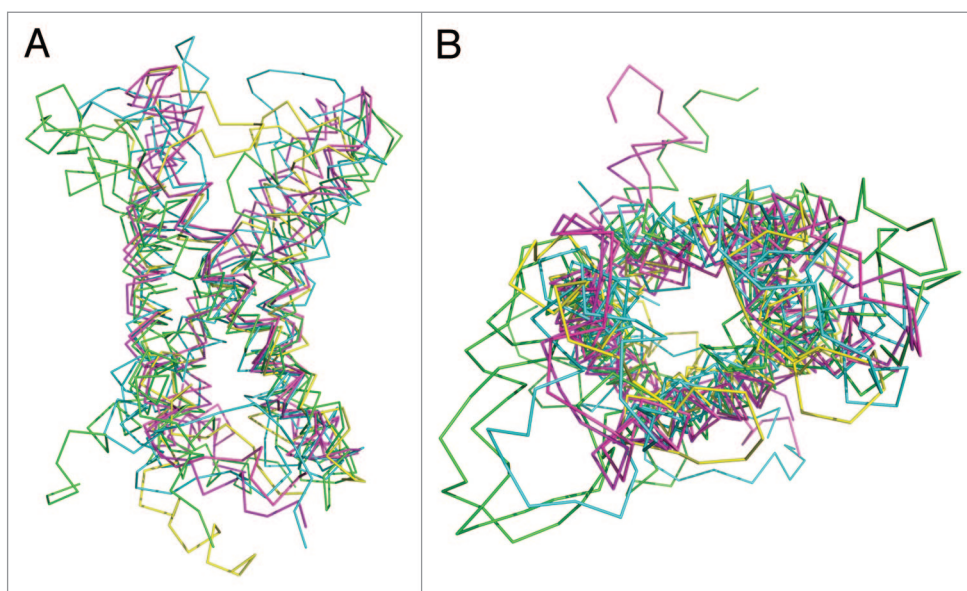


Figure 7. Best structural superposition of Hv1 models in the open conformation. Structure backbones are represented in ribbon, Hv1A and Hv1B are in green, R1-Hv1 and R2-Hv1 in cyan, R2D and R3D in magenta and Ci-Hv1 open in yellow. (A) Lateral view of superimposed structures (B) Top view.

with the exception of the interaction pair D160-R261. A docking conformation of the channel inhibitor 2GBI is presented as an additional validation for the model of the open conformation. In the interaction complex predicted by the docking simulation 2GBI is located close to F198 and interacting with the negative groups of E201, E219, and E222. Although Hong et al.⁷⁸ reported that F150 (the human equivalent to F198) plays a key role in 2GBI binding, this residue can be mutated for Alanine, which provokes a 360 fold increase in binding affinity for 2GBI.⁷⁸ F198 is clearly affecting how 2GBI can bind to the proton channel, but perhaps the finding of lower energy solutions in the docking of 2GBI vs. F198A mutant compared with docking against WT will provide a more robust validation of the model.

The third difference between the models proposed by Chamberlin et al.⁵ is that in their molecular dynamics simulations water wires through the channel were observed to have a transient existence. The longest living continuous water wire exist for 200–300 ps at most in 100 ns of simulation, and the average lifetime of a continuous water wire in the open state was ~6 ps. Based on this simulation, it is improbable that permeation occurs only by means of a water wire mechanism. Thus, it follows that titratable residues would participate. The authors, however, did not suggest possible candidates.

Based on their models, Chamberlin et al.⁵ proposed that a hydrophobic plug and salt-bridge network would function as the gates for Hv1 channel, which are formed in the closed conformation and disrupted in the open one. With models of both open and closed states it is possible to simulate the channel gating. The simulation was performed by a 100 ns targeted molecular dynamics, suggesting possible interactions during gating and allowing calculations of gating charge.

Major Convergences and Divergences between Models

Although 6 out of 7 models of the open proton channel use the same template (2R9R coordinates of Kv1.2–Kv2.1 paddle chimera) there is a large structural divergence between models (Fig. 7; Table 5). The most divergent structure is unsurprisingly the model *Ci-Hv1 closed*. Hv1A is the most different open channel model, while R2D and R3D constitute the most similar couple of structures, with an RMSD of only 3.3. It is worth noting how different the models proposed by the same group can be (Fig. 7; Table 5), which highlights how complex is to model the native and yet unknown structure of proton channels in the open conformation.

As can be seen in Table 5 *Ci-Hv1 closed* model is far from the crystallographic structure of the closed conformation (mHv1cc), which is consequence of the need to use low identity models as templates. But, what happens with the open conformation models? These models are expected to differ from the closed conformation (Table 5); however, most of the differences between the open and the closed conformations are expected to be caused by variations in the S4 segment. That is why we compared the coordinates of trans-membrane segments S1 to S3 of open state models and the closed state structure mHv1cc (Table 5). The best RMSD are not smaller than 5.8, which means that the conformations of S1 to S3 segments significantly differ between open state models and the closed structure. There are two possible explanations for this fact, first there could be a change in the relative orientation of S1, S2 and S3 segments during channel opening, which is a probable situation or second, all the models are inaccurate.

Table 5. Structural comparison of proton channel models

Models	Hv1A	Hv1B	R1-Hv1	R2-Hv1	R2D	R3D	Ci-Hv open	Ci-Hv closed	mHv1cc	MHv1cc S1-S3
Hv1A	–	–	–	–	–	–	–	–	–	–
Hv1B	8.0	–	–	–	–	–	–	–	–	–
R1-Hv1	8.1	7.1	–	–	–	–	–	–	–	–
R2-Hv1	7.0	5.4	5.7	–	–	–	–	–	–	–
R2D	8.8	6.5	6.6	4.5	–	–	–	–	–	–
R3D	7.7	5.2	5.7	3.9	3.3	–	–	–	–	–
Ci-Hv1 open	8.9	7.6	6.7	6.1	7.2	6.1	–	–	–	–
Ci-Hv1 closed	13.8	12.1	12.8	11.0	10.5	10.9	11.3	–	–	–
mHv1cc	13.5	10.7	8.4	7.0	6.9	7.1	8.1	8.5	–	–
mHv1cc S1-S3	7.4	5.8	6.6	5.9	5.8	5.8	6.2	7.0	0	–

RMSD values (Angstroms), considering Ca atoms of equivalent residues in superimposed structures, are reported. The structure of full, or just the first three trans-membrane segments, of the mHv1cc chimera in the closed conformation were included in the comparison. The RMSD values of the comparison between the Ci-Hv1 closed model and the mHv1cc structures are highlighted.

All open channel models, except *Ci-Hv1 open*, support the idea that permeation occurs by a Grotthuss mechanism through a relative stable water wire. However, current data are not conclusive on this aspect, and the possibility that some titratable group of the channel participate in the proton transfer chain, as was proposed by Chamberlin et al.,⁵ has not yet been discarded.

Model R2D support the role assigned to D122 (D160 in *Ciona intestinalis*) as the selectivity filter. In this model, D122 is in the extracellular compartment interacting with R208. Most of the models are coincident in positioning D122 where it is interacting with the second or the third Arg of the voltage sensor. D122 is in the extracellular vestibule for most models, with the exception of R1-Hv1, where D122 is the intracellular vestibule interacting with R211.

There is a consensus between models in the role played by E153 and D174 (E201 and D222 in *Ciona intestinalis*) as important residues to stabilize Hv1 closed conformation, and E119 and D185 (E167 and D233 in *Ciona intestinalis*) in stabilizing the open conformation, in both cases through electrostatic interactions with Arginines residues from S4 segment.

Sadly, none of the models provide a clue about the localization of pH sensor in Hv1 channel. This remains as one of the most interesting unsolved questions in the field.

Concluding Remarks

Structural models of the open conformation of proton channel although perhaps inaccurate to a certain extent, have allowed the interpretation of diverse experimental data, as well as, the design of new experiments and the creation of new structural models. Due to the lack of similar templates, there is a high structural divergence between proposed models. Existing experimental data does not make it possible to completely favor a particular model over the others. Until the structure of a closer homolog or, hopefully, the proton channel itself in the open conformation is resolved, Hv1 modeling will remain as an open task.

Disclosure of Potential Conflicts of Interest

No potential conflicts of interest were disclosed.

Acknowledgments

We would like to thank Francesco Tombola, Thomas E DeCoursey, Régis Pomès, Kethika Kulleperuma, Peter Larsson, Feng Qiu, David Clapham and I. Scott Ramsey for giving us the structural coordinates of their proton channel models, which facilitated and enriched the present study. This work was supported by FONDECYT Grants 1120802 (to C.G.), 1110430 (to R.L.) and ANILLO Grant ACT1104 (to C.G.). The Centro Interdisciplinario de Neurociencia de Valparaíso is a Millennium Institute supported by the Millenium Initiative of the Ministerio de Economía, Fomento y Turismo of Chile.

References

- Khalili-Araghi F, Tajkhorshid E, Roux B, Schulten K. Molecular dynamics investigation of the ω -current in the Kv1.2 voltage sensor domains. *Biophys J* 2012; 102:258-67; PMID:22339862; <http://dx.doi.org/10.1016/j.bpj.2011.10.057>
- Pathak MM, Yarov-Yarovsky V, Agarwal G, Roux B, Barth P, Kohout S, Tombola F, Isacoff EY. Closing in on the resting state of the Shaker K(+) channel. *Neuron* 2007; 56:124-40; PMID:17920020; <http://dx.doi.org/10.1016/j.neuron.2007.09.023>
- Long SB, Campbell EB, MacKinnon R. Crystal structure of a mammalian voltage-dependent Shaker family K⁺ channel. *Science* 2005; 309:897-903; PMID:16002581; <http://dx.doi.org/10.1126/science.1116269>
- Yarov-Yarovsky V, Baker D, Catterall WA. Voltage sensor conformations in the open and closed states in ROSETTA structural models of K(+) channels. *Proc Natl Acad Sci U S A* 2006; 103:7292-7; PMID:16648251; <http://dx.doi.org/10.1073/pnas.0602350103>
- Chamberlin A, Qiu F, Rebolledo S, Wang Y, Noskov SY, Larsson HP. Hydrophobic plug functions as a gate in voltage-gated proton channels. *Proc Natl Acad Sci USA* 2013; 111:E273-82; PMID:24379371
- Ramsey IS, Mokrab Y, Carvacho I, Sands ZA, Sansom MS, Clapham DE. An aqueous H⁺ permeation pathway in the voltage-gated proton channel Hv1. *Nat Struct Mol Biol* 2010; 17:869-75; PMID:20543828; <http://dx.doi.org/10.1038/nsmb.1826>
- Chen X, Wang Q, Ni F, Ma J. Structure of the full-length Shaker potassium channel Kv1.2 by normal-mode-based X-ray crystallographic refinement. *Proc Natl Acad Sci U S A* 2010; 107:11352-7; PMID:20534430; <http://dx.doi.org/10.1073/pnas.1000142107>
- Payandeh J, Scheuer T, Zheng N, Catterall WA. The crystal structure of a voltage-gated sodium channel. *Nature* 2011; 475:353-8; PMID:21743477; <http://dx.doi.org/10.1038/nature10238>
- Tao X, Lee A, Limapichat W, Dougherty DA, MacKinnon R. A gating charge transfer center in voltage sensors. *Science* 2010; 328:67-73; PMID:20360102; <http://dx.doi.org/10.1126/science.1185954>
- Jiang Y, Lee A, Chen J, Ruta V, Cadene M, Chait BT, MacKinnon R. X-ray structure of a voltage-dependent K⁺ channel. *Nature* 2003; 423:33-41; PMID:12721618; <http://dx.doi.org/10.1038/nature01580>
- Tang L, Gamal El-Din TM, Payandeh J, Martinez GQ, Heard TM, Scheuer T, Zheng N, Catterall WA. Structural basis for Ca(2+) selectivity of a voltage-gated calcium channel. *Nature* 2014; 505:56-61; PMID:24270805; <http://dx.doi.org/10.1038/nature12775>
- Wood ML, Schow EV, Freitas JA, White SH, Tombola F, Tobias DJ. Water wires in atomistic models of the Hv1 proton channel. *Biochim Biophys Acta* 2012; 1818:286-93; PMID:21843503; <http://dx.doi.org/10.1016/j.bbame.2011.07.045>
- Kulleperuma K, Smith SME, Morgan D, Musset B, Holyoake J, Chakrabarti N, Cherny VV, DeCoursey TE, Pomès R. Construction and validation of a homology model of the human voltage-gated proton channel hHV1. *J Gen Physiol* 2013; 141:445-65; PMID:23530137; <http://dx.doi.org/10.1085/jgp.201210856>
- Long SB, Tao X, Campbell EB, MacKinnon R. Atomic structure of a voltage-dependent K⁺ channel in a lipid membrane-like environment. *Nature* 2007; 450:376-82; PMID:18004376; <http://dx.doi.org/10.1038/nature06265>
- Payandeh J, Gamal El-Din TM, Scheuer T, Zheng N, Catterall WA. Crystal structure of a voltage-gated sodium channel in two potentially inactivated states. *Nature* 2012; 486:135-9; PMID:22678296
- Tsai C-J, Tani K, Irie K, Hiroaki Y, Shimomura T, McMillan DG, Cook GM, Schertler GFX, Fujiyoshi Y, Li X-D. Two alternative conformations of a voltage-gated sodium channel. *J Mol Biol* 2013; 425:4074-88; PMID:23831224; <http://dx.doi.org/10.1016/j.jmb.2013.06.036>
- Zhang X, Ren W, DeCaen P, Yan C, Tao X, Tang L, Wang J, Hasegawa K, Kumasaka T, He J, et al. Crystal structure of an orthologue of the NaChBac voltage-gated sodium channel. *Nature* 2012; 486:130-4; PMID:22678295
- Byerly L, Meech R, Moody W Jr. Rapidly activating hydrogen ion currents in perfused neurones of the snail, *Lymnaea stagnalis*. *J Physiol* 1984; 351:199-216; PMID:6086903
- Barish ME, Baud C. A voltage-gated hydrogen ion current in the oocyte membrane of the axolotl, *Ambystoma*. *J Physiol* 1984; 352:243-63; PMID:6086909
- Thomas RC, Meech RW. Hydrogen ion currents and intracellular pH in depolarized voltage-clamped snail neurones. *Nature* 1982; 299:826-8; PMID:7133121; <http://dx.doi.org/10.1038/299826a0>
- DeCoursey TE. Hydrogen ion currents in rat alveolar epithelial cells. *Biophys J* 1991; 60:1243-53; PMID:1722118; [http://dx.doi.org/10.1016/S0006-3495\(91\)82158-0](http://dx.doi.org/10.1016/S0006-3495(91)82158-0)
- DeCoursey TE, Cherny VV. Potential, pH, and arachidonate gate hydrogen ion currents in human neutrophils. *Biophys J* 1993; 65:1590-8; PMID:7506066; [http://dx.doi.org/10.1016/S0006-3495\(93\)81198-6](http://dx.doi.org/10.1016/S0006-3495(93)81198-6)
- Bernheim L, Krause RM, Baroffio A, Hamann M, Kaelin A, Bader CR. A voltage-dependent proton current in cultured human skeletal muscle myotubes. *J Physiol* 1993; 470:313-33; PMID:7508503
- Demaurex N, Grinstein S, Jaconi M, Schlegel W, Lew DP, Krause KH. Proton currents in human granulocytes: regulation by membrane potential and intracellular pH. *J Physiol* 1993; 466:329-44; PMID:7692041
- Ramsey IS, Moran MM, Chong JA, Clapham DE. A voltage-gated proton-selective channel lacking the pore domain. *Nature* 2006; 440:1213-6; PMID:16554753; <http://dx.doi.org/10.1038/nature04700>
- Sasaki M, Takagi M, Okamura Y. A voltage sensor-domain protein is a voltage-gated proton channel. *Science* 2006; 312:589-92; PMID:16556803; <http://dx.doi.org/10.1126/science.1122352>
- DeCoursey TE. Voltage-gated proton channels: what's next? *J Physiol* 2008; 586:5305-24; PMID:18801839; <http://dx.doi.org/10.1113/jphysiol.2008.161703>
- Iovannisci D, Illek B, Fischer H. Function of the HVCN1 proton channel in airway epithelia and a naturally occurring mutation, M91T. *J Gen Physiol* 2010; 136:35-46; PMID:20548053; <http://dx.doi.org/10.1085/jgp.200910379>
- Decoursey TE. Voltage-gated proton channels and other proton transfer pathways. *Physiol Rev* 2003; 83:475-579; PMID:12663866
- Musset B, Morgan D, Cherny VV, MacGlashan DW Jr., Thomas LL, Ríos E, DeCoursey TE. A pH-stabilizing role of voltage-gated proton channels in IgE-mediated activation of human basophils. *Proc Natl Acad Sci U S A* 2008; 105:11020-5; PMID:18664579; <http://dx.doi.org/10.1073/pnas.0800886105>
- Ramsey IS, Ruchti E, Kaczmarek JS, Clapham DE. Hv1 proton channels are required for high-level NADPH oxidase-dependent superoxide production during the phagocyte respiratory burst. *Proc Natl Acad Sci U S A* 2009; 106:7642-7; PMID:19372380; <http://dx.doi.org/10.1073/pnas.0902761106>
- Henderson LM, Chappell JB, Jones OT. The superoxide-generating NADPH oxidase of human neutrophils is electrogenic and associated with an H⁺ channel. *Biochem J* 1987; 246:325-9; PMID:2825632
- Lishko PV, Borchkina IL, Fedorenko A, Kirichok Y. Acid extrusion from human spermatozoa is mediated by flagellar voltage-gated proton channel. *Cell* 2010; 140:327-37; PMID:20144758; <http://dx.doi.org/10.1016/j.cell.2009.12.053>
- Musset B, Clark RA, DeCoursey TE, Petheo GL, Geiszt M, Chen Y, Cornell JE, Eddy CA, Brzyski RG, El Jamali A. NOX5 in human spermatozoa: expression, function, and regulation. *J Biol Chem* 2012; 287:9376-88; PMID:22291013; <http://dx.doi.org/10.1074/jbc.M111.314955>
- Capasso M, Bhamrah MK, Henley T, Boyd RS, Langlais C, Cain K, Dinsdale D, Pulford K, Khan M, Musset B, et al. HVCN1 modulates BCR signal strength via regulation of BCR-dependent generation of reactive oxygen species. *Nat Immunol* 2010; 11:265-72; PMID:20139987; <http://dx.doi.org/10.1038/ni.1843>
- Wang Y, Li SJ, Wu X, Che Y, Li Q. Clinicopathological and biological significance of human voltage-gated proton channel Hv1 protein overexpression in breast cancer. *J Biol Chem* 2012; 287:13877-88; PMID:22367212; <http://dx.doi.org/10.1074/jbc.M112.345280>
- Wu L-J, Wu G, Akhavan Sharif MR, Baker A, Jia Y, Fahey FH, Luo HR, Feener EP, Clapham DE. The voltage-gated proton channel Hv1 enhances brain damage from ischemic stroke. *Nat Neurosci* 2012; 15:565-73; PMID:22388960; <http://dx.doi.org/10.1038/nn.3059>
- Tombola F, Ulbrich MH, Isacoff EY. The voltage-gated proton channel Hv1 has two pores, each controlled by one voltage sensor. *Neuron* 2008; 58:546-56; PMID:18498736; <http://dx.doi.org/10.1016/j.neuron.2008.03.026>
- Koch HP, Kurokawa T, Okochi Y, Sasaki M, Okamura Y, Larsson HP. Multimeric nature of voltage-gated proton channels. *Proc Natl Acad Sci U S A* 2008; 105:9111-6; PMID:18583477; <http://dx.doi.org/10.1073/pnas.0801553105>
- Lee SY, Letts JA, MacKinnon R. Dimeric subunit stoichiometry of the human voltage-dependent proton channel Hv1. *Proc Natl Acad Sci U S A* 2008; 105:7692-5; PMID:18509058; <http://dx.doi.org/10.1073/pnas.0803277105>
- Lee S-Y, Letts JA, MacKinnon R. Functional reconstitution of purified human Hv1 H⁺ channels. *J Mol Biol* 2009; 387:1055-60; PMID:19233200; <http://dx.doi.org/10.1016/j.jmb.2009.02.034>
- Musset B, Decoursey T. Biophysical properties of the voltage gated proton channel H(V)1. *Wiley Interdiscip Rev Membr Transp Signal* 2012; 1:605-20; PMID:23050239; <http://dx.doi.org/10.1002/wmts.55>
- DeCoursey TE. Voltage-gated proton channels. *Cell Mol Life Sci* 2008; 65:2554-73; PMID:18463791; <http://dx.doi.org/10.1007/s00018-008-8056-8>
- Kuno M, Aoki H, Morihata H, Sakai H, Mori H, Sawada M, Ondo S. Temperature dependence of proton permeation through a voltage-gated proton channel. *J Gen Physiol* 2009; 134:191-205; PMID:19720960; <http://dx.doi.org/10.1085/jgp.200910213>
- DeCoursey TE, Cherny VV. Temperature dependence of voltage-gated H⁺ currents in human neutrophils, rat alveolar epithelial cells, and mammalian phagocytes. *J Gen Physiol* 1998; 112:503-22; PMID:9758867; <http://dx.doi.org/10.1085/jgp.112.4.503>
- Seoh SA, Sigg D, Papazian DM, Bezanilla F. Voltage-sensing residues in the S2 and S4 segments of the Shaker K⁺ channel. *Neuron* 1996; 16:1159-67; PMID:8663992; [http://dx.doi.org/10.1016/S0896-6273\(00\)80142-7](http://dx.doi.org/10.1016/S0896-6273(00)80142-7)

47. Aggarwal SK, MacKinnon R. Contribution of the S4 segment to gating charge in the Shaker K⁺ channel. *Neuron* 1996; 16:1169-77; PMID:8663993; [http://dx.doi.org/10.1016/S0896-6273\(00\)80143-9](http://dx.doi.org/10.1016/S0896-6273(00)80143-9)
48. Schoppa NE, McCormack K, Tanouye MA, Sigworth FJ. The size of gating charge in wild-type and mutant Shaker potassium channels. *Science* 1992; 255:1712-5; PMID:1553560; <http://dx.doi.org/10.1126/science.1553560>
49. Tombola F, Ulbrich MH, Kohout SC, Isacoff EY. The opening of the two pores of the Hv1 voltage-gated proton channel is tuned by cooperativity. *Nat Struct Mol Biol* 2010; 17:44-50; PMID:20023640; <http://dx.doi.org/10.1038/nsmb.1738>
50. Gonzalez C, Koch HP, Drum BM, Larsson HP. Strong cooperativity between subunits in voltage-gated proton channels. *Nat Struct Mol Biol* 2010; 17:51-6; PMID:20023639; <http://dx.doi.org/10.1038/nsmb.1739>
51. Mannuzzu LM, Moronne MM, Isacoff EY. Direct physical measure of conformational rearrangement underlying potassium channel gating. *Science* 1996; 271:213-6; PMID:8539623; <http://dx.doi.org/10.1126/science.271.5246.213>
52. Ruta V, Chen J, MacKinnon R. Calibrated measurement of gating-charge arginine displacement in the KvAP voltage-dependent K⁺ channel. *Cell* 2005; 123:463-75; PMID:16269337; <http://dx.doi.org/10.1016/j.cell.2005.08.041>
53. Larsson HP, Baker OS, Dhillon DS, Isacoff EY. Transmembrane movement of the shaker K⁺ channel S4. *Neuron* 1996; 16:387-97; PMID:8789953
54. Gonzalez C, Rebolledo S, Perez ME, Larsson HP. Molecular mechanism of voltage sensing in voltage-gated proton channels. *J Gen Physiol* 2013; 141:275-85; PMID:23401575; <http://dx.doi.org/10.1085/jgp.201210857>
55. Papazian DM, Shao XM, Seoh SA, Mock AF, Huang Y, Wainstock DH. Electrostatic interactions of S4 voltage sensor in Shaker K⁺ channel. *Neuron* 1995; 14:1293-301; PMID:7605638; [http://dx.doi.org/10.1016/0896-6273\(95\)90276-7](http://dx.doi.org/10.1016/0896-6273(95)90276-7)
56. Tiwari-Woodruff SK, Lin MA, Schulteis CT, Papazian DM. Voltage-dependent structural interactions in the Shaker K(+) channel. *J Gen Physiol* 2000; 115:123-38; PMID:10653892; <http://dx.doi.org/10.1085/jgp.115.2.123>
57. Lin MC, Hsieh JY, Mock AF, Papazian DM. R1 in the Shaker S4 occupies the gating charge transfer center in the resting state. *J Gen Physiol* 2011; 138:155-63; PMID:21788609; <http://dx.doi.org/10.1085/jgp.201110642>
58. Long SB, Tao X, Campbell EB, MacKinnon R. Atomic structure of a voltage-dependent K⁺ channel in a lipid membrane-like environment. *Nature* 2007; 450:376-82; PMID:18004376; <http://dx.doi.org/10.1038/nature06265>
59. Tao X, Lee A, Limapichat W, Dougherty DA, MacKinnon R. A gating charge transfer center in voltage sensors. *Science* 2010; 328:67-73; PMID:20360102; <http://dx.doi.org/10.1126/science.1185954>
60. Magrane M, Consortium U. UniProt Knowledgebase: a hub of integrated protein data. *Database (Oxford)* 2011; 2011:bar009.
61. Li SJ, Zhao Q, Zhou Q, Unno H, Zhai Y, Sun F. The role and structure of the carboxyl-terminal domain of the human voltage-gated proton channel Hv1. *J Biol Chem* 2010; 285:12047-54; PMID:20147290; <http://dx.doi.org/10.1074/jbc.M109.040360>
62. Takeshita K, Sakata S, Yamashita E, Fujiwara Y, Kawanabe A, Kurokawa T, Okochi Y, Matsuda M, Narita H, Okamura Y, et al. X-ray crystal structure of voltage-gated proton channel. *Nat Struct Mol Biol* 2014; (Forthcoming); PMID:24584463; <http://dx.doi.org/10.1038/nsmb.2783>
63. Ravna AW, Sylte I. Homology modeling of transporter proteins (carriers and ion channels). *Methods Mol Biol* 2012; 857:281-99; PMID:22323226; http://dx.doi.org/10.1007/978-1-61779-588-6_12
64. Liu T, Tang GW, Capriotti E. Comparative modeling: the state of the art and protein drug target structure prediction. *Comb Chem High Throughput Screen* 2011; 14:532-47; PMID:21521153; <http://dx.doi.org/10.2174/138620711795767811>
65. Martin AC, MacArthur MW, Thornton JM. Assessment of comparative modeling in CASP2. *Proteins* 1997; (Suppl 1): 14-28; PMID:9485491; [http://dx.doi.org/10.1002/\(SICI\)1097-0134\(1997\)1+<14::AID-PROT4>3.0.CO;2-O](http://dx.doi.org/10.1002/(SICI)1097-0134(1997)1+<14::AID-PROT4>3.0.CO;2-O)
66. Xiang Z. Advances in homology protein structure modeling. *Curr Protein Pept Sci* 2006; 7:217-27; PMID:16787261; <http://dx.doi.org/10.2174/13892030677452312>
67. Dalton JA, Jackson RM. An evaluation of automated homology modelling methods at low target template sequence similarity. *Bioinformatics* 2007; 23:1901-8; PMID:17510171; <http://dx.doi.org/10.1093/bioinformatics/btm262>
68. Venclovas C, Margelevicius M. Comparative modeling in CASP6 using consensus approach to template selection, sequence-structure alignment, and structure assessment. *Proteins* 2005; 61(Suppl 7):99-105; PMID:16187350; <http://dx.doi.org/10.1002/prot.20725>
69. Altschul SF, Gish W, Miller W, Myers EW, Lipman DJ. Basic local alignment search tool. *J Mol Biol* 1990; 215:403-10; PMID:2231712
70. Boratyn GM, Schäffer AA, Agarwala R, Altschul SF, Lipman DJ, Madden TL. Domain enhanced lookup time accelerated BLAST. *Biol Direct* 2012; 7:12; PMID:22510480; <http://dx.doi.org/10.1186/1745-6150-7-12>
71. Forrest LR, Tang CL, Honig B. On the accuracy of homology modeling and sequence alignment methods applied to membrane proteins. *Biophys J* 2006; 91:508-17; PMID:16648166; <http://dx.doi.org/10.1529/biophysj.106.082313>
72. Jacobson M, Sali A. Comparative Protein Structure Modeling and its Applications to Drug Discovery. *Annu Rep Med Chem* 2004; 39:259-76; [http://dx.doi.org/10.1016/S0065-7743\(04\)39020-2](http://dx.doi.org/10.1016/S0065-7743(04)39020-2)
73. Musset B, Smith SME, Rajan S, Cherny VV, Sujai S, Morgan D, DeCoursey TE. Zinc inhibition of monomeric and dimeric proton channels suggests cooperative gating. *J Physiol* 2010; 588:1435-49; PMID:20231140; <http://dx.doi.org/10.1113/jphysiol.2010.188318>
74. Musset B, Smith SME, Rajan S, Morgan D, Cherny VV, DeCoursey TE. Aspartate112 is the selectivity filter of the human voltage-gated proton channel. *Nature* 2011; 480:273-7; PMID:22020278; <http://dx.doi.org/10.1038/nature10557>
75. Ginalski K. Comparative modeling for protein structure prediction. *Curr Opin Struct Biol* 2006; 16:172-7; PMID:16510277; <http://dx.doi.org/10.1016/j.sbi.2006.02.003>
76. Morgan D, Musset B, Kulleperuma K, Smith SME, Rajan S, Cherny VV, Pomès R, DeCoursey TE. Peregrination of the selectivity filter delineates the pore of the human voltage-gated proton channel hHV1. *J Gen Physiol* 2013; 142:625-40; PMID:24218398; <http://dx.doi.org/10.1085/jgp.201311045>
77. Chowdhury S, Chanda B. Free-energy relationships in ion channels activated by voltage and ligand. *J Gen Physiol* 2013; 141:11-28; PMID:23250866; <http://dx.doi.org/10.1085/jgp.201210860>
78. Hong L, Pathak MM, Kim IH, Ta D, Tombola F. Voltage-sensing domain of voltage-gated proton channel Hv1 shares mechanism of block with pore domains. *Neuron* 2013; 77:274-87; PMID:23352164; <http://dx.doi.org/10.1016/j.neuron.2012.11.013>
79. Livingstone CD, Barton GJ. Protein sequence alignments: a strategy for the hierarchical analysis of residue conservation. *Comput Appl Biosci* 1993; 9:745-56; PMID:8143162